Effect of the resonant magnetic perturbation on the plasma parameters in COMPASS tokamak's divertor region

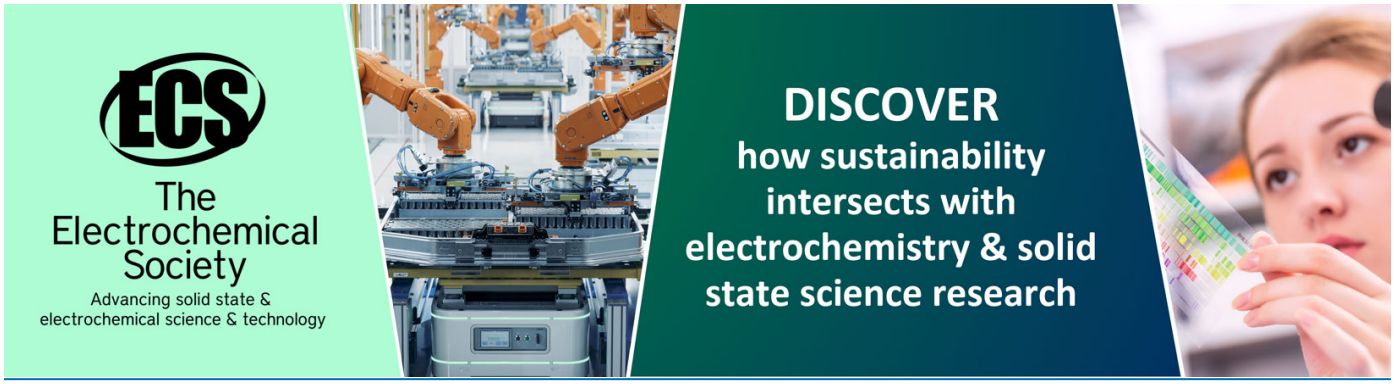

IOP Conf. Series: Journal of Physics: Conf. Series **982** (2018) 012001 doi:10.1088/1742-6596/982/1/012001

Effect of the resonant magnetic perturbation on the plasma parameters in COMPASS tokamak's divertor region

M Dimitrova[1,2,5], P Cahyna[1], M Peterka[1,3], E Hasan[2,4], Tsv K Popov[4], P Ivanova[2], E Vasileva[2], R Panek[1], J Cavalier[1], J Seidl[1], T Markovic[1,3], J Havlicek[1], R Dejarnac[1], V Weinzettl[1], P Hacek[1,3], M Tomes[1,3], the COMPASS team and the EUROfusion MST1 team*

[1] Institute of Plasma Physics, The Czech Academy of Sciences, Za Slovankou 3, 182 00 Prague 8, Czech Republic
[2] Emil Djakov Institute of Electronics, Bulgarian Academy of Sciences, 72, Tsarigradsko Chaussee, 1784 Sofia, Bulgaria
[3] Faculty of Mathematics and Physics, Charles University, Ke Karlovu 3, 2116 Prague 2, Czech Republic
[4] Faculty of Physics, St. Kliment Ohridski University of Sofia, 5, James Bourchier Blvd., 1164 Sofia, Bulgaria
* see http://www.euro-fusionscipub.org/mst1

E-mail: dimitrova@ipp.cas.cz

Abstract. The resonant magnetic perturbation (RMP) has proven to be a useful way to suppress edge-localized modes that under certain conditions can damage the device by the large power fluxes carried from the bulk plasma to the wall. The effect of RMP on the L-mode plasma parameters in the divertor region of the COMPASS tokamak was studied using the array of 39 Langmuir probes embedded into the divertor target. The current-voltage (*IV*) probe characteristics were processed by the first-derivative probe technique to obtain the plasma potential and the electron energy distribution function (EEDF) which was approximated by a bi-Maxwellian EEDF with a low-energy (4-6 eV) fraction and a high-energy (11-35 eV) one, the both factions having similar electron density. Clear splitting was observed during the RMP pulse in the low-field-side scrape-off-layer profiles of the floating potential U_{fl} and the ion saturation current density J_{sat}; these two quantities were obtained both by direct continuous measurement and by evaluation of the *IV* characteristics of probes with swept bias. The negative peaks of U_{fl} induced by RMP spatially overlaps with the local minima of J_{sat} (and n_e) rather than with its local maxima which is partly caused by the spatial variation of the plasma potential and partly by the changed shape of the EEDF. The effective temperature of the whole EEDF is not correlated with the negative peaks of U_{fl}, and the profile of the parallel power flux density shows secondary maxima due to RMP which mimic those of J_{sat}.

1. Introduction

During tokamak operation in high energy confinement mode (H-mode), the plasma experiences periodic relaxations of the edge transport barrier known as edge-localized modes (ELMs). The

[5] To whom any correspondence should be addressed.

resonant magnetic perturbation (RMP) has proven to be a useful way to suppress ELMs that under certain conditions can damage the device by the large power fluxes carried from the bulk plasma to the wall [1]. Successful mitigation or suppression of the type I ELMs by RMP has already been demonstrated on a number of devices [2-4]. Variations of plasma parameters in the scrape-of layer (SOL) are sensitive indicators of the effects of RMP and its screening by the plasma response [5, 6]. The COMPASS tokamak [7] is equipped with a system of RMP coils with a variety of possible configurations [8], two of which (both with top-bottom symmetry) have recently been utilized for measurements of the magnetic response of ohmic L-mode plasmas to the applied RMP field [9]. Here we report on the effect of this RMP on plasma parameters in the divertor region in these experiments.

The divertor probe system in COMPASS consists of 39 single graphite Langmuir probes embedded in the divertor target and provides profiles of the data measured with a typical spatial resolution in the poloidal direction down to 5 mm. During the experiments, the probes were operated in two different regimes: in a continuous measurement of the floating potential U_{fl}, or in a measurement with a swept probe bias. The current-voltage (*IV*) characteristics obtained during the swept regime were processed using the first-derivative probe technique (FDPT) [10-12], which allows evaluation of the plasma potential and the real electron energy distribution function (EEDF).

2. Results and discussion

2.1 Continuous measurement of the U_{fl} by the divertor probes.

In this regime, the signal from the divertor probes was recorded directly by the COMPASS tokamak DAQ with no additional electronics nor a power supply. As an example, figure 1a presents the temporal profile of the floating potential on the divertor probes, L-mode discharge #9684 (plasma current I_{pl} = 210 kA, toroidal magnetic field B_T = 1.15 T, edge safety factor q_{95} = 3.8 and line-average density n_e^{avr} = 5×10^{19} m^{-3}); the yellow line is the current in the RMP coils (with maximum at +3.5 kA), the black solid lines represent the position of the strike points determined from the magnetic equilibrium reconstruction code EFIT++.

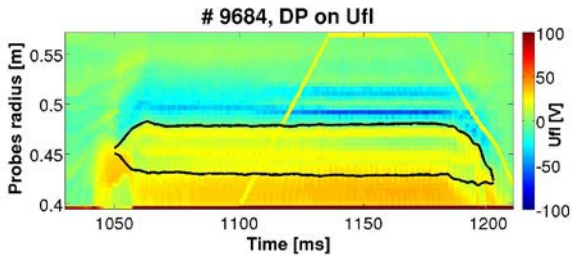

Figure 1 a. Temporal evolution of the floating potential on the divertor probes.

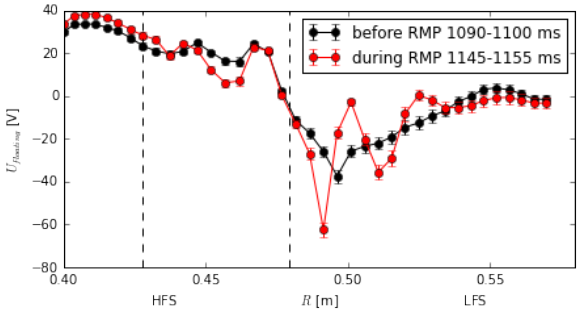

Figure 1 b. Poloidal profile of the floating potential before and during RMP in shot #9684.

Figure 1b shows the poloidal profiles of U_{fl} before RMP (black curve) and during RMP at 1150 ms (red curve), the dashed lines indicate the positions of the strike points at 1150 ms. One can see the asymmetry of the floating potential profile − positive values on the high-field side (HFS) and negative on the low-field side (LFS). In contrast to the regime without RMP, during RMP clear splitting of the strike points was observed in the U_{fl} signal as a spatial oscillation in the LFS SOL. This is in qualitative agreement with the striped structure of the visible light emission at the divertor as observed by the fast visible light camera (figure 2) as well as with the lobes intersecting the divertor (figure 3) as predicted by a vacuum model of the last closed flux surface invariant manifolds [13].

The measurements during discharge #9684 were performed at a fixed position of the strike points (black lines, figure 1a). To increase the spatial resolution of the measurements, the X-point was swept, moving the plasma from the LFS towards the HFS. The temporal evolution of the U_{fl} profile during the experiment with swept X-point is shown in figure 4, with the same meaning of yellow and black

solid lines as in figure 1a. The profile changes immediately both at the start and the end of the RMP pulse.

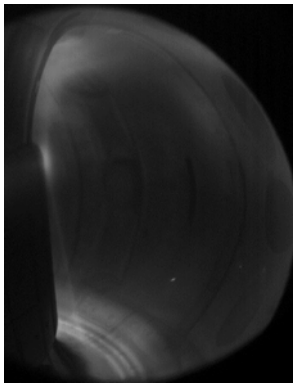

Figure 2. Splitting of the outer strike-point observed by a fast VIS camera.

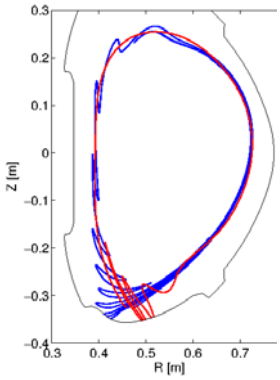

Figure 3. Vacuum model of the invariant manifold lobes in COMPASS.

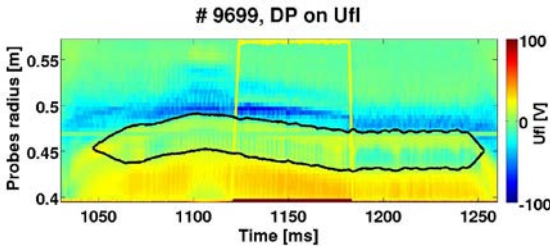

Figure 4. Temporal evolution of the floating potential on the divertor probes at swept strike points.

2.2 Swept divertor probes measurements.

To study the RMP influence on the plasma behavior during the movement of the X-point, other plasma parameters, such as the plasma potential, electron temperature and density, are of interest. For this purpose, the probes were biased with respect to the tokamak vessel by a +60 ÷ −160 V triangular voltage $U_p(t)$ swept at a frequency of 1 kHz by a KEPCO 100-4 M power supply. The probe bias $U_p(t)$ and probe current $I_p(t)$ were measured and the $I_p(U_p)$ probe characteristics were evaluated by FDPT.

As an example, figure 5 shows the results for U_{fl} and the ion saturation current density J_{sat} around position R_{osp} of the outer strike point during L-mode discharge #9694 (I_{pl} = 170 kA, B_T = 1.15 T, q_{95} = 3.8, $n_e^{avr} = 4.5\times10^{19}$ m^{-3} off-midplane configuration of the RMP: +4 kA [9]) at different times during the discharge, namely, at time 1100 ms before the RMP and at 1125 ms and 1150 ms during RMP. One can see clearly pronounced splitting in the measured quantities' poloidal profiles, with positions of the minima and maxima shifted in accordance with the X-point movement, i.e. appearing at a constant value of R- R_{osp}. The splitting is observed on LFS only, though some changes are present on HFS as well. Note that the precision of the R_{osp} (determined by EFIT++) is only approximately 1 cm.

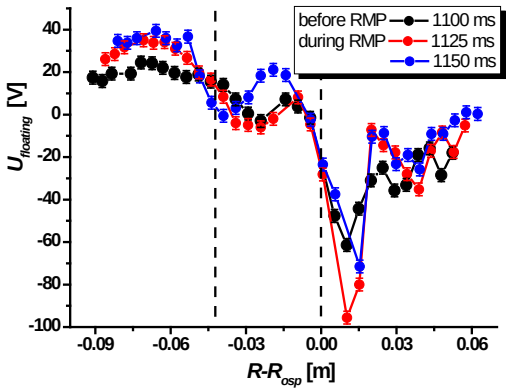

Figure 5 a. Poloidal profile of the floating potential before and during RMP.

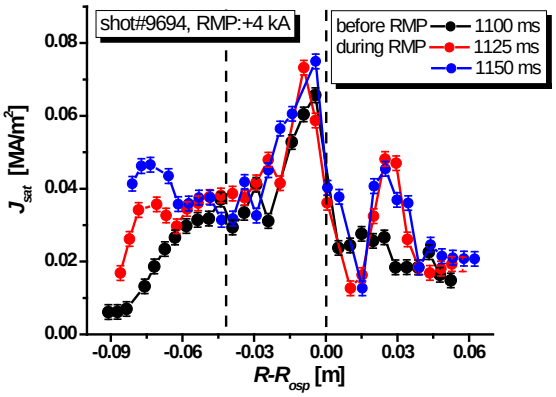

Figure 5 b. Poloidal profile of the ion saturation current density before and during RMP.

It is important to point out that the local minimum of U_{fl} occurs at the position of the local minimum of J_{sat}, which is contradictory to the common expectation that the interior of the intersecting

lobes should appear as negative peak of U_{fl} [14] as well as positive peak of the particle flux J_{sat}. This can be attributed to the SOL conditions in this COMPASS discharge being different from typical conditions in RMP experiments at larger devices, e.g. a high recycling divertor regime.

The profile of U_{fl} is influenced by the plasma potential U_{pl} and by the shape of EEDF (mostly by its high-energy tail); both can be obtained by the FDPT. In figure 6a we can see that the poloidal variation of U_{pl} can explain most of the variation of the U_{fl} except the large negative peak at the distance R - R_{osp} = 0.01 m.

The EEDFs obtained deviate from Maxwellian and can be approximated by bi-Maxwellian EEDFs with a low-energy (4-6 eV) electron fraction (triangles in figure 6 b) and a high-energy (11-35 eV) electron group (squares). Similar results were obtained in our previous investigations [11]; the presence of the low-energy group is attributed to the ionization process as confirmed by a model [12].

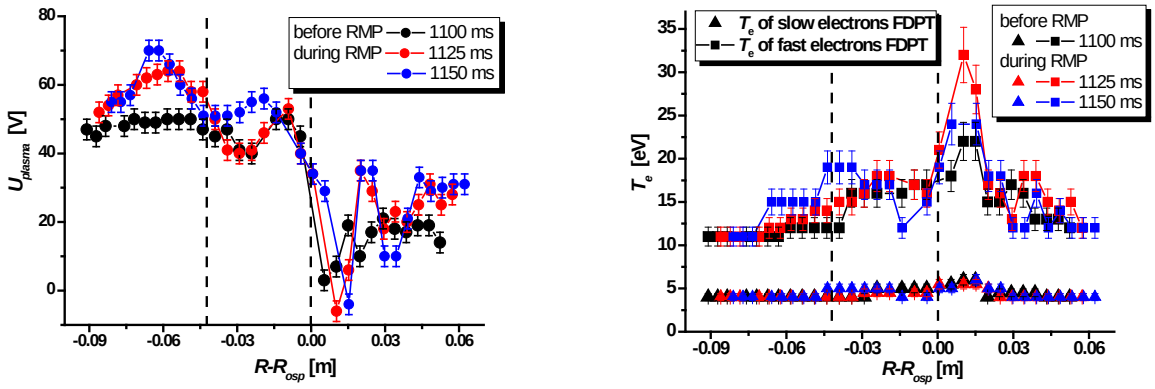

a) **b)**

Figure 6. Poloidal profile of the plasma potential **a)** and electron temperatures **b)** for discharge #9694

The splitting due to the RMP field is weakly pronounced on the electron temperature profiles as expected from the comparison between the profiles of U_{fl} and U_{pl}. The temperature of the high-energy electron group T_e^h increases by about 10 eV at the distance 0.01 m at time 1125 ms which explains the large negative peak of U_{fl}. The peak is less pronounced in the profile at 1150 ms, where the maximum is located in between two probes (the strike points were shifted towards the HFS).

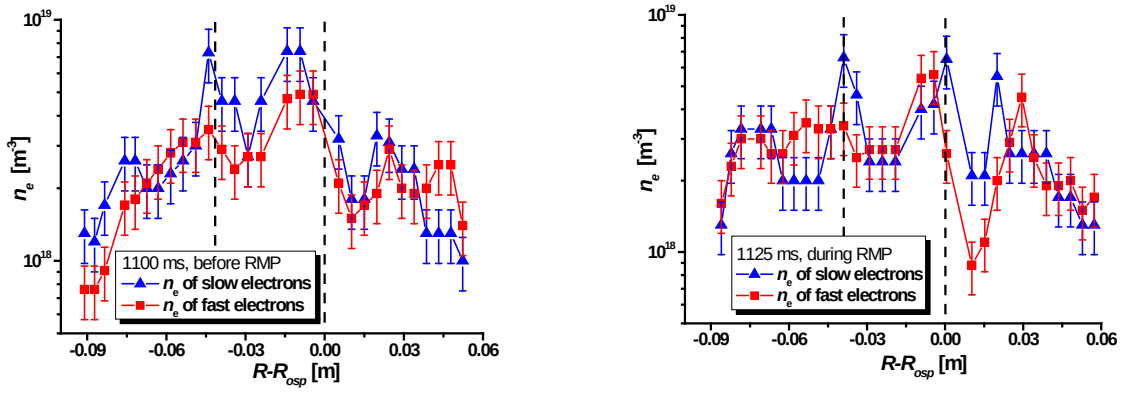

a) **b)**

Figure 7. Poloidal profile of the electron density **a)** before and **b)** during RMP, discharge #9694.

Evaluation of densities of both electron groups by the FDPT is hampered by a relatively larger error but we can distinguish the qualitative change between the profiles during RMP (figure 7 b) and before RMP (figure 7 a). The density of the high-energy electrons decreases after application of RMP by a factor of 2 at the distance 0.01 m which is clearly correlated with the increase of T_e^h. This is

consistent with the drop of J_{sat} at this position after application of RMP (figure 5 b). It is interesting to note that a local minimum of the density of both electron groups is present at this position also before the RMP pulse, although more difficult to distinguish in J_{sat} due to the linear scale.

The parallel power flux density can be calculated from the effective temperature T_e^{eff} which takes into account the temperatures and densities of both electron groups [12]:

$$Q_{||} \cong \gamma \cdot T_e^{eff} \, J_{sat} \tag{1}$$

Here γ is the sheath heat transition coefficient and its value is in the range of 11-24 depending on the ratio T_e^h / T_e^{eff} as proposed in [12] for the case of a bi-Maxwellian EEDF. The ion temperature T_i is less affected by atomic processes and thus typically higher than the electron temperature in the SOL; $T_i = T_e^h$ is assumed here for the power flux calculation. The ratio T_e^h / T_e^{eff} is presented in figure 8, the resulting parallel power flux in figure 9.

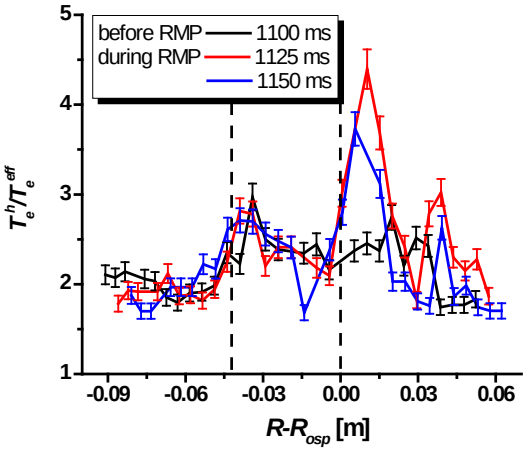

Figure 8. The ratio between the high-energy electron group temperature and the effective temperature.

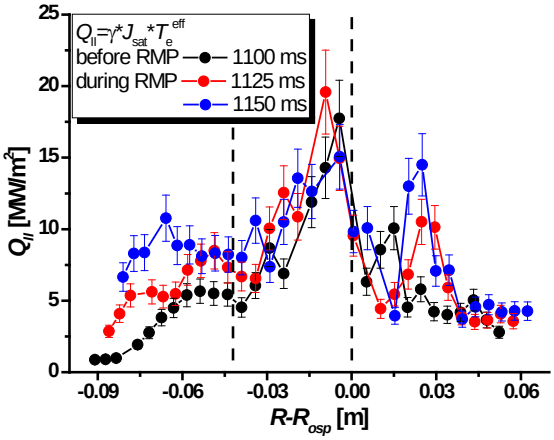

Figure 9. Poloidal distribution of the parallel power flux density $Q_{||}$.

A large effect of RMP on the T_e^h / T_e^{eff} ratio is observed at the distance 0.01 m, where the temperature of the high-energy electrons increases (figure 6 b) but their density decreases at the same time (figure 7 b) and thus the effective temperature remains the same. As expected, the negative peak of U_{fl} observed at this position is only related to the high-energy group and does not correlate with changes of the effective electron temperature. Therefore, the profile of the power flux density is dominated by the profile of J_{sat} and we can observe clear secondary maxima which mimic those on figure 5 b.

In experiments with negative polarity of the applied RMP field, reversal of the splitting pattern in the LFS divertor profiles is observed – the maxima appear at the locations of former minima and vice versa – but the relations between the profiles of individual plasma parameters remain analogical. The splitting was observed for both the on+off-midplane and off-midplane RMP configuration [9] with very similar results.

3. Conclusions

The effect of RMP on the L-mode plasma parameters in divertor region of the COMPASS tokamak was studied using the array of 39 Langmuir probes embedded into the divertor target. The probe *IV* characteristics were processed by the first-derivative probe technique to obtain the plasma potential and the EEDF which was approximated by a bi-Maxwellian EEDF with a low-energy (4-6 eV) fraction and a high-energy (11-35 eV) one, the both factions having similar electron density.

Clear splitting was observed during the RMP pulse in the LFS scrape-off-layer profiles of the floating potential U_{fl} and the ion saturation current density J_{sat}; these two quantities were obtained both by direct continuous measurement and by evaluation of the *IV* characteristics of probes with swept bias. Surprisingly, we observe that the negative peak of U_{fl} induced by RMP spatially overlaps with the local minimum of J_{sat} (and n_e) rather than with its local maximum. On one hand this is contradictory to the common expectation that the interior of the intersecting lobes should appear as negative peak of U_{fl} [14] as well as positive peak of the particle flux J_{sat}. On the other hand, the formation of divertor profiles depends to a large extent on the conditions in the SOL and particularly at the divertor target, which can vary substantially between different experiments and devices (such as high-recycling vs. low-recycling divertor).

The common interpretation that decreased U_{fl} should be attributed to increased electron temperature does not hold in all cases. In this work we show that most of the spatial variation of U_{fl} is caused by the variation of U_{pl} except for the largest negative peak induced by RMP. At the position of this negative U_{fl} peak, we observe an increase only in the temperature of the high-energy electron fraction but the relative share of this fraction decreases at the same time, and the effective temperature of the whole EEDF is thus not affected.

The profile of the parallel power flux density is influenced mainly by the profile of J_{sat} and therefore we can observe formation of secondary maxima at the LFS during the RMP pulse.

Acknowledgements

This research has been partially supported by International Atomic Energy Agency (IAEA) Research Contract No 17125/R0, R1 and R2 as a part of the IAEA CRP F13014 on "Utilisation of a Network of Small Magnetic Confinement Fusion Devices for Mainstream Fusion Research" 2014 IAEA Joint Experiment, by the Joint Research Project between the Institute of Plasma Physics of the CAS and the Institute of Electronics BAS BG, by the Czech Science Foundation grant No. 16-24724S and by MEYS project # LM2015045. This work has been also carried out within the framework of the EUROfusion Consortium and has received funding from the EURATOM research and training programme 2014-2018 under grant agreement No 633053 and the Co-fund by MEYS project number 8D15001. The views and opinions expressed herein do not necessarily reflect those of the European Commission.

References

[1] Loarte A et al 2014 *Nucl. Fusion* **54** 033007
[2] Liang Y et al 2007 *Phys. Rev. Lett.* **98** 265004
[3] Evans T E et al 2008 *Nucl. Fusion* **48** 024002
[4] Kirk A et al 2015 *Nucl. Fusion* **55** 043011
[5] Nardon E et al 2011 *J. Nucl. Mater.* **415** S914–S917
[6] Conway G D, Fietz S, Müller H W, Lunt T, Simon P, Suttrop W, Maraschek M, Happel T, Viezzer E and the ASDEX Upgrade Team 2015 *Plasma Phys. Control. Fusion* **57** 014035
[7] Panek R et al 2016 *Plasma Phys. Control. Fusion* **58** 014015
[8] Cahyna P, Panek R, Fuchs V, Krlin L, Becoulet M, Huysmans G and Nardon E 2009 *Nucl. Fusion* **49** 055024
[9] Markovic T et al 2016 *Nucl. Fusion* **56** 092010
[10] Popov Tsv K, Ivanova P I, Stockel J and Dejarnac R 2009 *Plasma Phys. Control. Fusion* **51** 065014
[11] Dimitrova M, Dejarnac R, Popov Tsv K, Ivanova P, Vasileva E, Kovačič J, Stöckel J, Havlicek J, Janky F and Panek R 2014 *Contrib. Plasma Phys*. **54** No. 3**,** 255
[12] Popov Tsv K et al 2015 *Plasma Phys. Control. Fusion* **57** 115011
[13] Cahyna P, Nardon E and JET EFDA Contributors 2011 *J. Nucl. Mater.* **415** S927–S931
[14] Watkins J G, Evans T E, Jakubowski M, Moyer R A, Schmitz O, Wingen A, Fenstermacher M E, Joseph I, Lasnier C J and Rudakov D L 2009 *J. Nucl. Mater.* **390–391** 839–842